Tech Science Press

Experimental and Theoretical Study on Bonding Properties between Steel Bar and Bamboo Scrimber

Xiangya Luo, Haiqing Ren and Yong Zhong[*]

Research Institute of Wood Industry, Chinese Academy of Forestry, Beijing, 100714, China
*Corresponding Author: Yong Zhong. Email: zhongyong108@163.com

Abstract: To further verify the feasibility of newly designed reinforced bamboo scrimber composite (RBSC) beams used in building construction, the bonding properties between steel bar and bamboo scrimber were investigated by anti-pulling tests. Results indicated that the anti-pulling mechanical properties were significantly correlated to the diameter, thread form and buried depth of steel bar, forming density of bamboo scrimber as well as the heat treatment of bamboo bundle. There were two failure modes for anti-pulling tests: the tensile fracture and pulling out of steel bar. Both the ultimate load and average shear strength of anti-pulling specimen could be increased greatly with the ribbed bar, high forming density of bamboo scrimber and un-heated bamboo bundle. Furthermore, a theoretical calculation model of the bonding interface between steel bar and bamboo scrimber was developed. Based on the theoretical calculation model, the change laws of normal stress of bamboo scrimber, and shear stress of glue layer along the buried depth of steel bar were revealed. This study is beneficial for the safety application of RBSC beams in building construction.

Keywords: Reinforced bamboo scrimber composite (RBSC); bonding properties; anti-pulling tests; theoretical calculation model

1 Introduction

It is well known that China has abundant bamboo resources accounting for about one-third of the world [1–3]. More than 40 genera and 500 species of bamboo are distributed mainly around Fujian, Zhejiang, Anhui provinces and so on. Moreover, bamboo is a fast-growing resource and can be harvest in 3~5 years [4–5]. Moso bamboo, as one of the greatest areas accounting for 71% in China, is becoming the most important bamboo specie as a construction material used in green buildings, because of its high yield, good physical and mechanical properties, and processing performance [6].

However, the natural bamboo used in building construction is restricted mainly due to the small diameter of bamboo culms and the high variability of mechanical properties. To resolve these problems, many bamboo-based composite products made by new manufacturing technology have been explored, such as glum bamboo, glue-laminated bamboo, bamboo strip, bamboo scrimber and so on [7–19]. Among them, bamboo scrimber has enormous advantages in green building construction due to its high manufacture efficiency, utilization and good mechanical strength [20–24], which is manufactured by using physical

treatment without any chemical and moving the inner and outer layers of bamboo. But the modulus of bamboo scrimber is low compared with its high strength, which leads to that the design bearing capacity of bamboo scrimber beam is controlled by its stiffness [1,25]. Therefore, a feasible method to improve the stiffness of bamboo scrimber beam is proposed by combining bamboo scrimber with other reinforcing materials such as steel, carbon fiber.

In our previous study [1], a newly designed reinforced bamboo scrimber composite (RBSC) beam has been developed and manufactured through a cold pressing process (Fig. 1). Both the ultimate load and stiffness of beams could significantly increase when the steel bar was used as the strengthen element. It is known that the bonding properties between steel bar and bamboo scrimber determine the improvement level of stiffness and strength for RBSC beam. In order to verify the feasibility of newly designed reinforced bamboo scrimber composite (RBSC) beams, i.e., the bonding properties between steel bar and bamboo scrimber, sixteen types of anti-pulling specimens with different configurations were manufactured.

Figure 1: Newly designed reinforced bamboo scrimber composite (RBSC) beams

This study aimed to investigate the effects of the diameter, thread form and buried depth of steel bar, forming density of bamboo scrimber as well as the heat treatment of bamboo bundle on the bonding properties (failure mode, ultimate load and average shear strength), and to propose a theoretical calculation model of the bonding interface between steel bar and bamboo scrimber to infer the normal stress and shear stress.
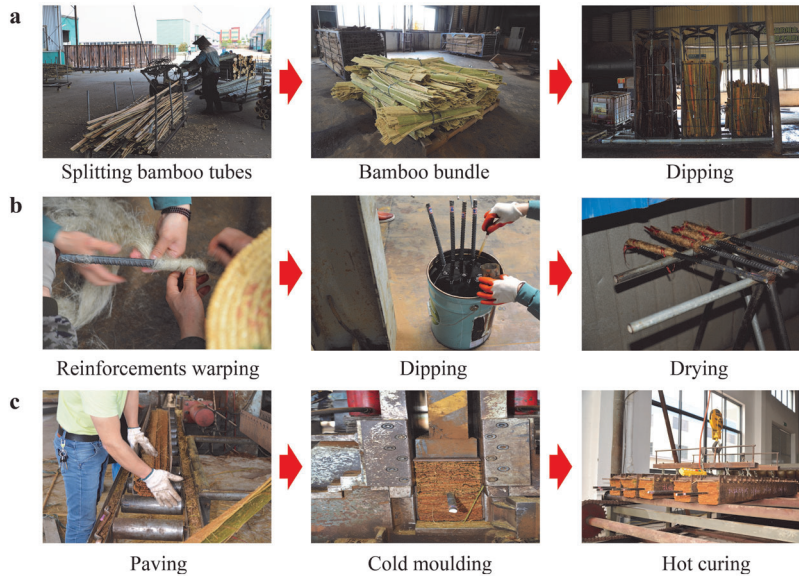
2 Materials and Methods

2.1 Materials

As shown in Fig. 2, the manufacturing process of anti-pulling specimen contains three main steps (a) preparation of the bamboo bundle; (b) preparation of the steel bar; (c) molding of the specimen.

First, the Moso bamboo (*Phyllostachys pubescens*) with age of 3~4 years, was harvested from Guangde county, Anhui province, in the southeast part of China. The range of these bamboo culms was 100~150 mm in average diameter and was 12~20 mm in average thickness. The bamboo culms were cut into long pieces, and then were split into two semicircular or more bamboo tubes with the removal of inter nodes. Without moving the inner layer and outer layer, the bamboo tubes were passed through a rolling machine along the grain direction, and then were flattened along the longitudinal fiber direction to produce the oriented bamboo bundle [16,20]. To evaluate the effects of heat treatment of bamboo bundle on the anti-pull properties, some of bamboo bundles were heated for 140 min by steam at a temperature of 175°C (Tab. 1). Both unheated and heated bamboo bundles were immersed in resin for about 10~15 min at room temperature (20°C), and then were dried for 8 h at 45~50°C.

Second, two types of steel bars including ribbed and un-ribbed were used to investigate the influences of thread form of steel bar on the anti-pull properties. Both ribbed and un-ribbed steel bar used is a common

Figure 2: Manufacturing process of anti-pulling specimen contains three main steps: (a) preparation of the bamboo bundle; (b) preparation of the steel bar; (c) molding of the specimen

Table 1: Types of anti-pulling specimens

Number	Types of steel bar			Types of bamboo scrimber	
	Diameter (mm)	Thread form	Buried depth (mm)	Forming density (g/cm^3)	Bamboo bundle
A-01	8	Ribbed	200	0.9	Un-heated
A-02	8	Ribbed	250	0.9	Un-heated
A-03	12	Ribbed	200	0.9	Un-heated
A-04	12	Ribbed	250	0.9	Un-heated
A-05	16	Ribbed	200	0.9	Un-heated
A-06	16	Ribbed	250	0.9	Un-heated
A-07	16	Un-ribbed	200	0.9	Un-heated
A-08	16	Un-ribbed	250	0.9	Un-heated
A-09	16	Ribbed	200	0.9	Heated
A-10	16	Ribbed	250	0.9	Heated
A-11	16	Ribbed	200	1.0	Un-heated
A-12	16	Ribbed	250	1.0	Un-heated
A-13	16	Ribbed	200	1.0	Heated
A-14	16	Ribbed	250	1.0	Heated
A-15	16	Ribbed	200	1.1	Un-heated
A-16	16	Ribbed	250	1.1	Un-heated

construction material with Q235-B grade. The strength grade has a nominal yield strength of 235 MPa and modulus of elasticity of 206 GPa provided by the manufacturer. For enhancing the bonding properties between steel bar and bamboo scrimber, the steel bar were wrapped up by linen with a thickness of 2~3 mm. Thereafter, the steel bar were immersed in resin for about 3~5 min at room temperature (20°C), and then were dried for 8 h at a temperature 45~50°C.

Finally, after the preparation of bamboo bundle and steel bar, both them were paved along the grain direction and cold pressed for 3 min, and then were hot cured for 12 h at a temperature of 130~140°C. The adhesive resin used in manufacture process was a commercially available low molecular weight phenol formaldehyde resin (PF16L510) with a solid content of 6~49%, viscosity of 20~40 CPS, 10~11 pH, and dissolve ability of 7 times in water, supplied by Beijing Dynea Chemical Industry Co., Ltd.

2.2 Design of Anti-Pulling Specimens

Sixteen types of anti-pulling specimens with a cross sectional dimension of 150 mm × 150 mm, were designed for mechanical test as shown in Tab. 1. The anti-pulling specimens (A-01~A-16) contained three kinds of diameters (8, 12 and 16 mm), two kinds of thread forms (ribbed and un-ribbed), two kinds of buried depths (200 and 250 mm) for steel bar, two kinds of bamboo bundles (un-heated and heated) and three kinds of forming densities (0.9, 1.0 and 1.1 g/cm³) for bamboo scrimber. Among them, the specimens A-01~A-10 as the low forming density was 0.9 g/cm³, A-11~A-14 as the medium forming density was 1.0 g/cm³, and A-15 and A-16 as the high forming density was 1.1 g/cm³. In addition, the bamboo bundles used in specimens A-01~A-08, A-11, A-12, A-15 and A-16 as the un-heated type were heated for 140 min by steam at a temperature of 175°C in preparation of bamboo element (Fig. 2) while the other specimens were defined as the un-heated type. All the anti-pulling specimen are shown in Fig. 3.


Figure 3: Anti pulling specimens after failure

The mechanical properties of individual materials, such as compressive strength (CS) and compressive modulus (CM) of the bamboo scrimber, as well as the yield strength of steel bar, were evaluated according to the Chinese national standards. The mean value and standard deviation of mechanical properties are presented in Tab. 2.

2.3 Anti-Pulling Tests

The anti-pulling tests were conducted by a universal testing machine (Model 301, Jinan Shi Jin Co., Ltd., China) with a load capacity 300 kN. The schematic drawing and photos of the anti-pulling tests were shown in Fig. 4.

Table 2: Mechanical properties of individual material

Individual materials	Mechanical properties		Specimens	Mean value/MPa	Standard deviation/MPa
bamboo scrimber composite (un-heated)	CS	0.9 g/cm^3	30	115.92	5.96
		1.0 g/cm^3	30	116.02	8.03
		1.1 g/cm^3	30	118.22	5.28
	CM	0.9 g/cm^3	30	16828	1470
		1.0 g/cm^3	30	19009	878
		1.1 g/cm^3	30	20794	1401
bamboo scrimber composite (heated)	CS	0.9 g/cm^3	30	97.64	7.99
		1.0 g/cm^3	30	100.54	5.12
	CM	0.9 g/cm^3	30	16134	1079
		1.0 g/cm^3	30	18331	1916
Steel	Yield strength		10	263.7	13.6
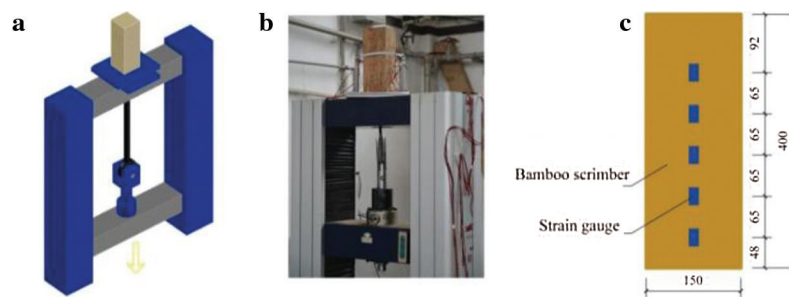
Figure 4: Anti pull-out test on specimens: (a) schematic drawing; (b) photo; (c) strain monitoring points of bamboo scrimber

In order to measure the strain distribution along the direction of buried depth of steel bar, ten strain gauges (Model: BX120-80AA, Xingtai Jin Li Co., Ltd., China) were symmetrically attached on the front and rear surfaces of each specimen (Fig. 4c). The data were collected simultaneously by the TDS-530 multi-channels data acquisition equipment (Earth Products China Co., Ltd., China). The specimens were loaded until failure at a loading speed 2 mm/min.

For the anti-pulling tests, the average shear strength ($\overline{\tau}$) of each specimen could be calculated as follows [26,27]:

$$\overline{\tau} = P_{max}/(\pi dl) \tag{1}$$

where P_{max} represents the ultimate load of specimens (N); d is the diameter of steel bar (mm); l is the buried depth of steel bar (mm).

3 Experimental Results

3.1 Failure Modes

Fig. 5 shows two failure modes for anti-pulling tests: (I) the tensile fracture of steel bar; (II) pulling out of steel bar, and all load-displacement curves for these failure modes. The load-displacement curves for model I contained four stages: linear elasticity stage, yield stage, hardening stage, and necking failure stage; while those for model II contained three stages: linear elasticity stage, non-linear stage, and failure stage over the maximum static friction force, as presented in Fig. 6.
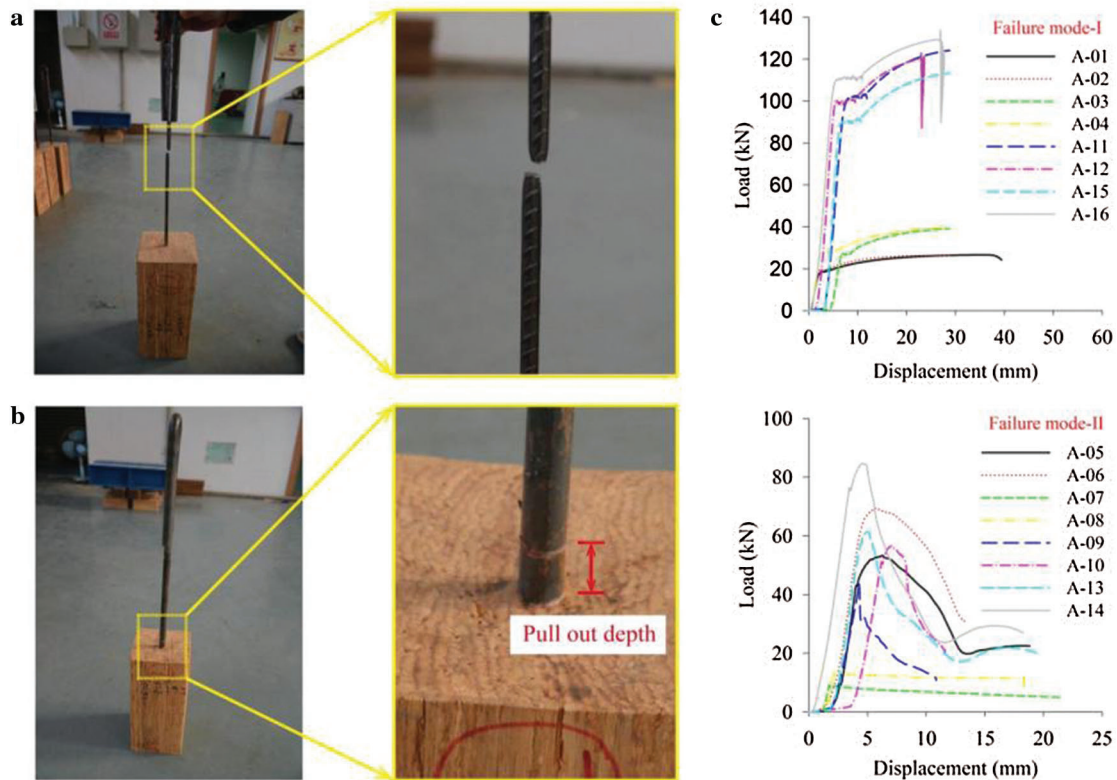
Figure 5: Failure modes for anti-pulling tests: (a) model I; (b) model II; (c) load-displacement curves

According to the analytical result of each specimen (Tab. 3), it could be found that the failure modes of anti-pulling tests were closely correlated to the diameter, thread form and buried depth of reinforcement, the forming density of bamboo scrimber as well as the heat treatment of bamboo bundle. Specimens with high forming density (A-15~A-16), small-diameter of steel bar (A-01~A-04), and un-heated bamboo bundle (A-11~A-12) presented the failure model I. The other specimens presented the failure model II, and had a ultimate bearing capacity lower than ultimate tension load of steel bar itself.
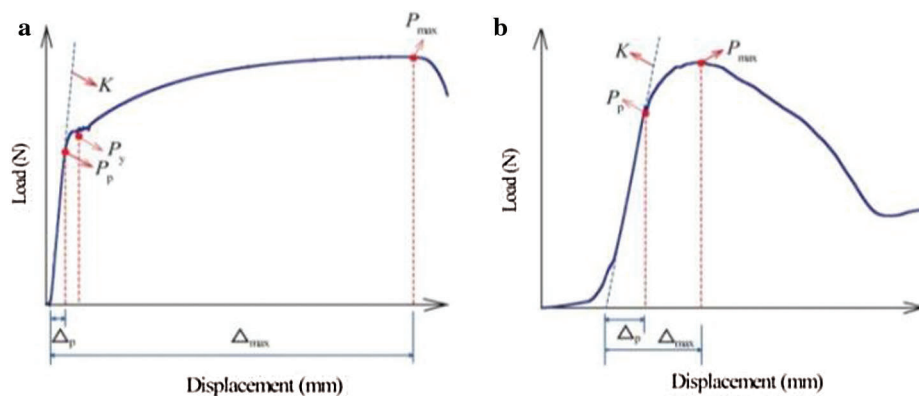
Figure 6: Mechanical properties of anti-pulling specimens: (a) model I; (b) model II. P_{max}—the ultimate load (N); Δ_{max}—the corresponding displacement at P_{max} (mm); P_p—theproportional limit load (N); Δ_p—the corresponding displacement at P_p (mm); P_y—the yield load (N); K—the stiffness of whole anti-pulling specimens (N/mm)

Table 3: Mechanical properties of anti-pulling specimens

Number	P_{max} (kN)	Δ_{max} (mm)	P_p (kN)	Δ_p (mm)	P_y (kN)	K (kN/mm)	$\bar{\tau}$ (MPa)	Failure modes
A-01	26.667	34.750	15.359	1.528	18.438	11.973	—	I
A-02	26.455	26.503	15.235	1.377	18.941	13.419	—	I
A-03	39.178	24.153	22.395	1.576	26.752	14.080	—	I
A-04	39.613	27.586	24.355	1.680	27.438	15.200	—	I
A-05	53.292	3.799	43.731	1.538	—	28.566	5.301	II
A-06	69.332	3.572	46.632	1.553	—	29.312	5.517	II
A-07	9.945	0.557	8.670	0.464	—	19.535	0.989	II
A-08	13.524	0.855	12.259	0.596	—	19.137	1.076	II
A-09	44.523	2.179	44.523	2.179	—	20.001	4.429	II
A-10	56.721	3.200	51.449	2.292	—	22.895	4.514	II
A-11	124.205	25.194	87.398	3.098	101.136	29.978	—	I
A-12	120.345	21.462	83.157	2.524	98.164	34.394	—	I
A-13	61.410	2.760	49.782	1.762	—	27.636	6.109	II
A-14	84.644	3.778	76.261	2.667	—	28.519	6.736	II
A-15	113.473	25.218	75.449	2.128	89.458	35.718	—	I
A-16	129.370	24.981	95.976	3.064	110.136	31.946	—	I

3.2 Ultimate Load and Average Shear Strength

The specimens for failure model II (Tab. 3), did not have slip damage and were thus not analysied in following process. Compared to the anti-pulling specimens with un-ribbed steel bar (A-05 *vs.* A-07, A-06 *vs.* A-08), it was found that both the ultimate load (P_{max}) and average shear strength ($\bar{\tau}$) of anti-pulling specimens could be significantly increased by using the ribbed steel bar. The P_{max}, $\bar{\tau}$, Δ_{max}, P_p, Δ_p, and K of specimen A-05 were respectively 4.36, 4.36, 5.82, 4.04, 2.31, 0.46 times higher than those of specimen A-07, while those of specimen A-06 were respectively 4.13, 4.13, 3.18, 2.80, 1.61, 0.53 times higher than those of specimen A-08. This was mainly because that the friction force, mechanical interaction between steel bar and bamboo scrimber can be increased by using the ribbed bar with a unsmooth surface [28–29].

Relative to the anti-pulling specimens with heated bamboo bundle (A-05 *vs.* A-09, A-06 *vs.* A-10), it was suggested that both the ultimate load (P_{max}) and average shear strength ($\bar{\tau}$) of anti-pulling specimens could be increased by using the un-heated bamboo bundle. The P_{max}, $\bar{\tau}$, Δ_{max}, and K of specimen A-05 were respectively 19.7%, 19.7%, 74.3%, 42.8% higher than those of specimen A-09, while those of specimen A-06 were respectively 22.2%, 22.2%, 11.6%, 28.0% higher than those of specimen A-10. However, the P_p of specimen A-05, A-06 with un-heated bamboo bundle was decrease by 1.8%, 9.4% than those of specimen A-09, A-10 with heated bamboo bundle. Similarly, the Δ_p of specimen A-05, A-06 with un-heated bamboo bundle was decrease by 29.4%, 32.2% than that of specimen A-09, A-10 with heated bamboo bundle. This phenomenon could be explained by that the heat treatment of bamboo bundle implemented an inverse effect on the mechanical strength of bamboo scrimber, which was consistent with the findings of [30–33].

Compared with the the anti-pulling specimens with low forming density (A-09 *vs.* A-13, A-10 *vs.* A-14), it was indicated that both the ultimate load (P_{max}) and average shear strength ($\bar{\tau}$) of anti-pulling specimens could be increased by using the high forming density. The P_{max}, $\bar{\tau}$, Δ_{max}, P_p and K of specimen A-13 were respectively 37.9%, 37.9%, 26.7%, 11.8%, 38.2% higher than those of specimen A-09, while those of specimen A-14 were respectively 49.2%, 49.2%, 18.1%, 48.2%, 24.6% higher than those of specimen A-10. But the Δ_p under different forming densities showed no apparent trend. This results were caused by the increasing of friction force, mechanical interaction between steel bar and bamboo scrimber when the forming density of bamboo scrimber was increased.

Besides, with the increase of buried depth of steel bar from 200 mm to 250 mm (A-05 *vs.* A-06, A-07 *vs.* A-08, A-09 *vs.* A-10 and A-13 *vs.* A-14), the ultimate load (P_{max}) could be significantly increased, but the K and $\bar{\tau}$ of anti-pulling specimens were nearly no change.

3.3 Load-Strain Curves of Bamboo Scrimber

To investigate the strain distribution along the buried depth of steel bar, the strains of five detection points on bamboo scrimber surface of anti-pulling specimens were plotted in Fig. 7.
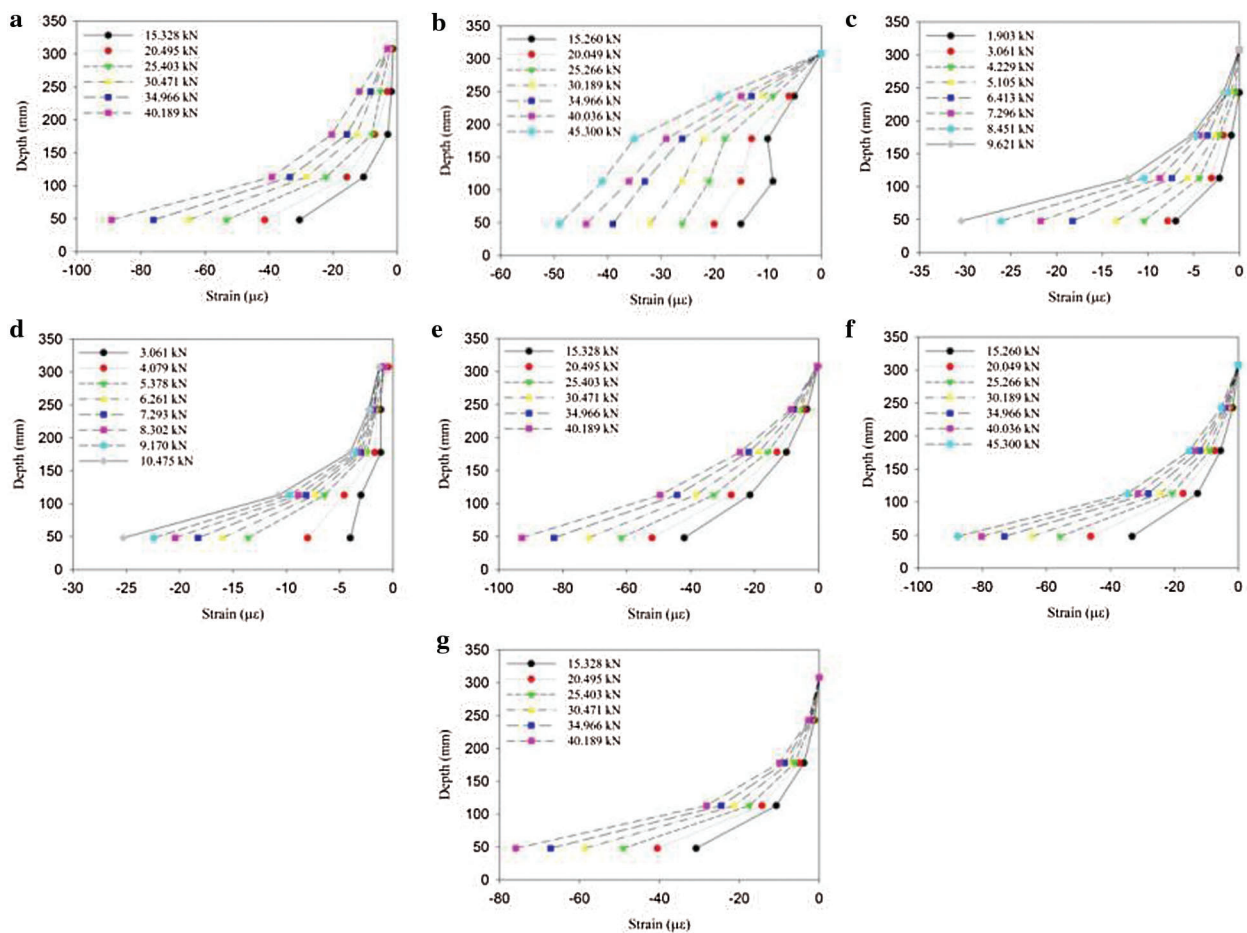
Figure 7: Strain distribution along the buried depth of steel bar under different loads: (a) A-05; (b) A-06; (c) A-07; (d) A-08; (e) A-09; (f) A-10; (g) A-13

Under different loads, the compression strains of all anti-pulling specimens along the buried depth of steel bar were nonlinear decrease. The maximum compression strain was at the starting point of buried depth, the minimum compression strain was at the ending point of buried depth and was almost equal to zero. Furthermore, by comparison of different anti-pulling specimens (A-05 *vs.* A-06, A-07 *vs.* A-08 and A-09 *vs.* A-10) under the same load condition, it was found that the compression strain at the same height for 250 mm buried depth was less than that for 200 mm buried depth.

4 Theoretical Analysis of Interfacial Bonding

4.1 Theoretical Calculation Model

To deeply investigate the interfacial bonding properties between bamboo scrimber and steel bar for anti-pulling specimens, a theoretical calculation model of interfacial bonding was developed, as shown in Fig. 8. In this model, the interfacial bonding contained three parts: steel bar, glue layer and bamboo scrimber. Based on above analysis (Fig. 5 and Tab. 3), the interfacial bonding was reliable before the ultimate load, and it is thus assumed that: (a) the normal stress of bamboo scrimber at the same height of cross section is equally distributed; (b) the interface between bamboo scrimber and steel bar meets the deformation compatibility. The interfacial bonding properties between bamboo scrimber and steel bar for anti-pulling specimens can be determined according to the material strength theory.
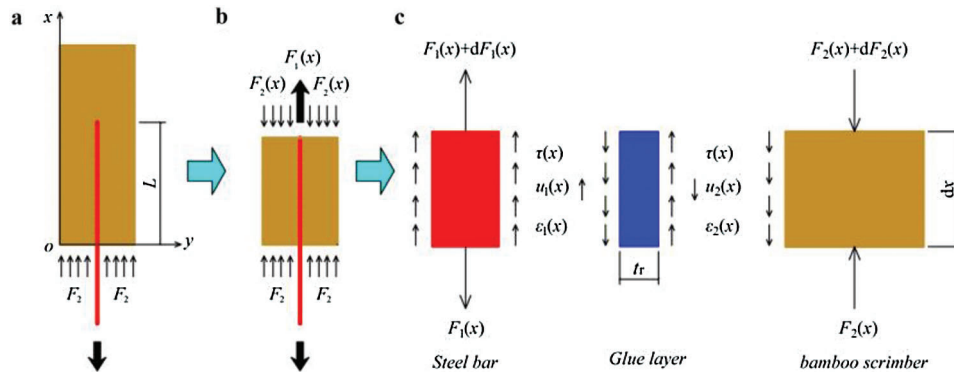
Figure 8: Mechanical analysis diagram: (a) whole elevation drawing of anti-pulling specimens; (b) element in calculus; (c) stress of bonding interface

According to the shear deformation of glue layer, the shear stress of bonding interface ($\tau(x)$) could be calculated as follows:

$$\tau(x) = G_r\gamma(x) \tag{2}$$

where G_r is the shear modulus of glue layer (MPa); $\gamma(x)$ is the shear strain of glue layer ($\mu\varepsilon$); x is the buried depth of steel bar (mm).

However, due to the unmeasurable thickness and shear modulus of the glue layer, $\tau(x)$ could not be directly calculated by Eq. (2), and should be calculated based on the analysis of bamboo scrimber. Therefore, the balance equation of bamboo scrimber could be expressed as:

$$F_2(x) - \tau(x)c_s dx = F_2(x) + dF_2(x) \tag{3}$$

$$dF_2(x) = (A_b - A_s)d\sigma_2(x) \tag{4}$$

where $F_2(x)$ is the force contributed by the whole cross section of bamboo scrimber (N); $\sigma_2(x)$ is the normal stress of bamboo scrimber at the same height (MPa); A_b is the whole section area of bamboo scrimber (mm^2); A_s is the section area of steel bar (mm^2); c_s is the circumference of steel bar (mm).

By substitution of Eq. (4) into Eq. (3), $\tau(x)$ could be expressed as:

$$\tau(x) = -\frac{(A_b - A_s)d\sigma_2(x)}{c_s dx} \tag{5}$$

From Eq. (5), it was found that to obtain the normal stress of bamboo scrimber ($\sigma_2(x)$) is the key to calculate $\tau(x)$. In order to get the analytic formula of $\sigma_2(x)$, it was assumed that the displacement changes of glue layer along x-axis, y axis are u (mm) and v (mm), respectively. The shear strain of glue layer ($\gamma(x)$) could be calculated by Eq. (6).

$$\gamma(x) = \frac{du}{dy} + \frac{dv}{dx} \tag{6}$$

By substitution of Eqs. (2) and (6) into Eq. (5), the formula could be expressed as:

$$\frac{d\sigma_2(x)}{dx} = -\frac{c_s G_r}{(A_b - A_s)}\left(\frac{du}{dy} + \frac{dv}{dx}\right) \tag{7}$$

After derivation calculus to above Eq. (7), the formula was transformed into Eq. (8).

$$\frac{d^2\sigma_2(x)}{dx^2} = -\frac{c_s G_r}{(A_b - A_s)}\left(\frac{d^2u}{dydx} + \frac{d^2v}{dx^2}\right) \tag{8}$$

Due to a thin thickness of glue layer, the displacement change of glue layer along y axis (v) was almost equal to zero. Therefore, the Eq. (8) could be simplified as:

$$\frac{d^2\sigma_2(x)}{dx^2} = -\frac{c_s G_r}{(A_b - A_s)}\frac{d^2u}{dydx} = \frac{c_s G_r}{(A_b - A_s)}\frac{\varepsilon_2(x) + \varepsilon_1(x)}{t_r} \tag{9}$$

where $\varepsilon_1(x)$ is the strain of steel bar along x axis ($\mu\varepsilon$); $\varepsilon_2(x)$ is the strain of bamboo scrimber along x axis ($\mu\varepsilon$); t_r is the thickness of glue layer (mm).

In addition, according to Fig. 8b, the balance equations could be also obtained:

$$\varepsilon_1(x) = \frac{F_1(x)}{A_s E_s} = \frac{F_2(x)}{A_s E_s} = \frac{(A_b - A_s)\sigma_2(x)}{A_s E_s} \tag{10}$$

$$\varepsilon_2(x) = \frac{\sigma_2(x)}{E_b} \tag{11}$$

where E_s, E_b is the elastic modulus of steel bar and bamboo scrimber (MPa), respectively.

By substitution of Eqs. (10) and (11) into Eq. (9), the formula which is a second-order differential equation, could be expressed as:

$$\frac{d^2\sigma_2(x)}{dx^2} - p\sigma_2(x) = 0 \tag{12}$$

$$p = \frac{c_s G_r}{t_r}\left(\frac{1}{A_s E_s} + \frac{1}{E_b(A_b - A_s)}\right) \tag{13}$$

It was infered that $p > 0$ according to the calculation result by Eq. (13). Thus, the general solutions of normal stress of bamboo scrimber ($\sigma_2(x)$) could be expressed as:

$$\sigma_2(x) = C_1 e^{\sqrt{p}x} + C_2 e^{-\sqrt{p}x} \tag{14}$$

The constant coefficients C_1 and C_2 was determined based on the loading boundary conditions: (a) $x = 0$, $\sigma_2(0) = F_1/(A_b\text{-}As)$; $x = L$, $\sigma_2(L) = 0$. And Eq. (14) could be changed into:

$$\sigma_2(x) = \frac{F_1(e^{\sqrt{p}L}e^{-\sqrt{p}x} - e^{-\sqrt{p}L}e^{\sqrt{p}x})}{(A_b - A_s)(e^{\sqrt{p}L} - e^{-\sqrt{p}L})} \tag{15}$$

Combining with Eqs. (15) and (5), the analytical formula for shear stress of bonding interface ($\tau(x)$) could be as follow:

$$\tau(x) = -\frac{F_1(\sqrt{p}e^{\sqrt{p}L}e^{-\sqrt{p}x} + \sqrt{p}e^{-\sqrt{p}L}e^{\sqrt{p}x})}{c_s(e^{\sqrt{p}L} - e^{-\sqrt{p}L})} \tag{16}$$

Consider the Eqs. (15) and (16), where p is unknown parameter and could not be directly calculated by Eq. (13) due to the unmeasurable thickness (t_r) and shear modulus (G_r) of glue layer. Consequently, an indirectly method was developed to solve the parameter p, where the parameter p was estimated by the least squares fitting of Eq. (15) with the actual measured normal stress data of bamboo scrimber ($\sigma_2(x)$) (Fig. 7). And the indirectly solving method was then proved in following analysis whether or not $\tau(x)$ could be accurately predicted.

4.2 Fitting Results of Parameter p

According to the above indirectly solving method, a calculation program for least squares fitting was developed to determine the parameter p by use of Matlab 7 software. And then the ratio of shear modulus (G_r) to thickness (t_r) of glue layer could be calculated by Eq. (13). The calculation results are shown in Tab. 4.

Table 4: Fitting results by least squares fitting method

| Number	p	G_r/t_r (N/mm^3)	τ_{max} (MPa)
A-05	1.292×10^{-4}	105.232	12.303
A-06	1.278×10^{-4}	104.044	15.691
A-07	3.844×10^{-5}	31.297	1.450
A-08	3.642×10^{-5}	29.656	1.790
A-09	9.446×10^{-5}	76.905	8.963
A-10	8.783×10^{-5}	71.507	10.765
A-13	1.656×10^{-4}	134.809	15.894
A-14	1.656×10^{-4}	134.809	21.723

Notice: τ_{max} is the maximum shear stress distributed in the bonding interface.

By comparison of the anti-pulling specimens with un-ribbed and ribbed steel bar (A-05 *vs.* A-07, A-06 *vs.* A-08), it was found that the parameter p could be significantly increased by using the ribbed steel bar. The parameter p of specimen A-05 was 2.36 times higher than that of specimen A-07, while that of specimen

A-06 was 2.51 times higher than that of specimen A-08. Besides, compared to heated bamboo bundle of anti-pulling specimens, it was indicated that the parameter p could be increased by using the un-heated bamboo bundle, and were increased by 36.8%, 45.5% for A-05 vs. A-09 and A-06 vs. A-10, respectively. And the parameter p could be also increased by using the high forming density, which was increased by 75.3%, 88.5% for A-09 vs. A-13 and A-10 vs. A-14. But with the increase of buried depth for steel bar from 200 mm to 250 mm (A-05 vs. A-06, A-07 vs. A-08, A-09 vs. A-10 and A-13 vs. A-14), the parameter p had slight decrease and was less than 8% change. The main leading cause of these phenomenons have be explained in above chapter 3.2.

4.3 Normal Stress Distribution of Bamboo Scrimber

Based on the the fitting results of parameter p (Tab. 4), the normal stress distribution of bamboo scrimber ($\sigma_2(x)$) along the buried depth could be infered by Eq. (15), as shown in Fig. 9.
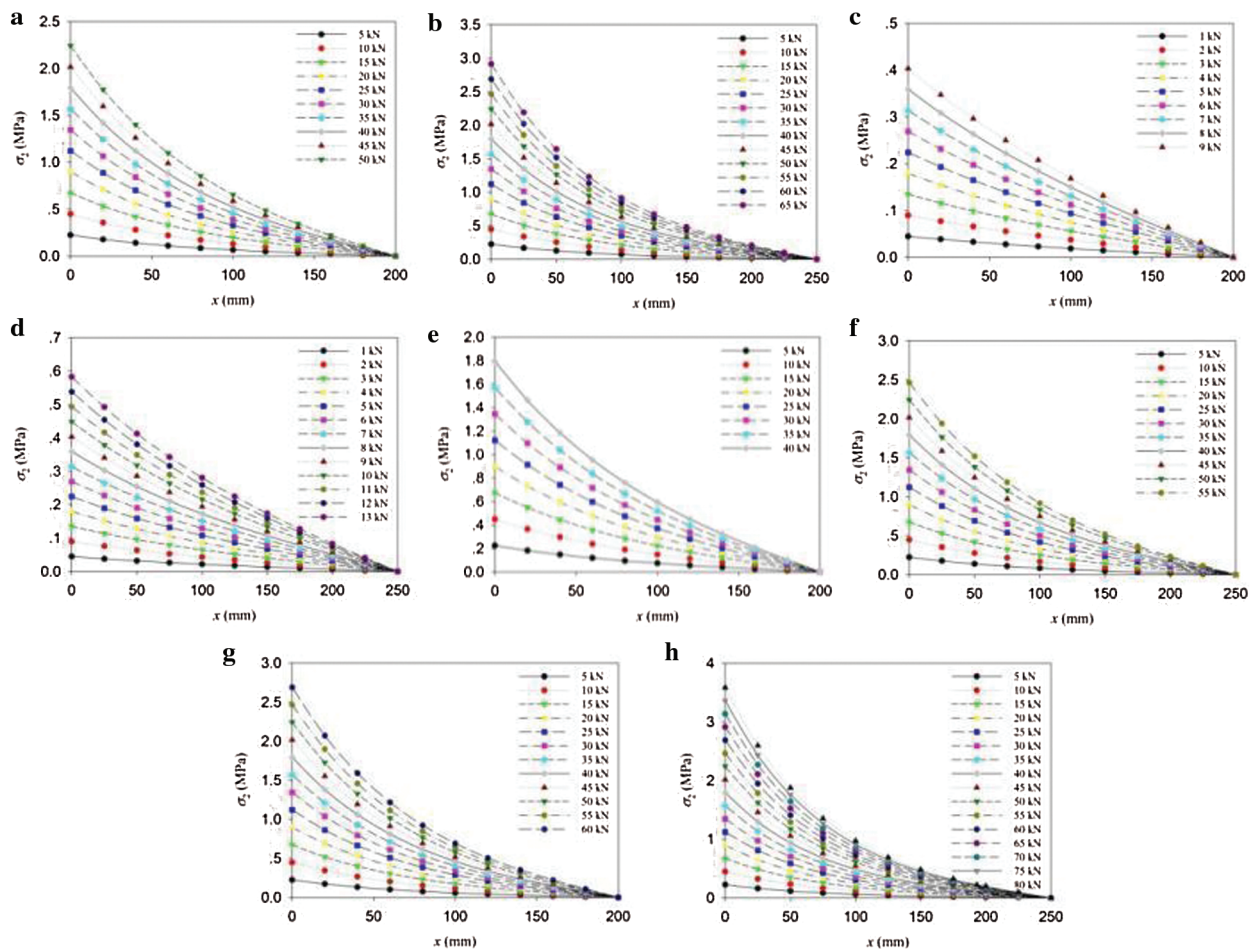
Figure 9: Normal stress distribution of bamboo scrimber along the buried depth for steel bar: (a) A-05; (b) A-06; (c) A-07; (d) A-08; (e) A-09; (f) A-10; (g) A-13; (h) A-14

It was observed that the normal stress of bamboo scrimber ($\sigma_2(x)$) decreases nonlinearly from the maximum value at the start $x = 0$ top to zero at the end ($x = L$). The more parameter p (Figs. 9a, 9b, 9g and 9h), the more nonlinear decreasing in $\sigma_2(x)$ was (A-05, A-06, A-13 and A-14). But for the smaller

parameter p of A-07 and A-08, $\sigma_2(x)$ showed linear decrease. The numerical results (Fig. 9) were shown to be in good agreement with the actual experimental results presented by Fig. 7, and the feasibility of above indirectly method was proved.

4.4 Shear Stress Distribution of Bonding Interface

The shear stress distribution of bonding interface ($\tau(x)$) along the buried depth is shown in Fig. 10, which is calculated by Eq. (16) with the the fitting results of parameter p (Tab. 4).

Fitting results indicated that $\tau(x)$ first increase rapidly and then tended to stable with the increase of buried depth. The inhomogeneous distribution of $\tau(x)$ decreased when the p was smaller, e.g., A-07 and A-08. Additionally, The maximum shear stress (τ_{max}) could be calculated by substitution of the parameter p (Tab. 4), ultimate load (p_{max}) of anti-pulling specimens into Eq. (16). With the increase of buried depth from 200 mm into 250 mm, τ_{max} decreased by 27.5%, 23.4%, 20.1% and 36.7% for A-05 vs. A-06, A-07 vs. A-08, A-09 vs. A-10, A-13 vs. A-14, respectively.
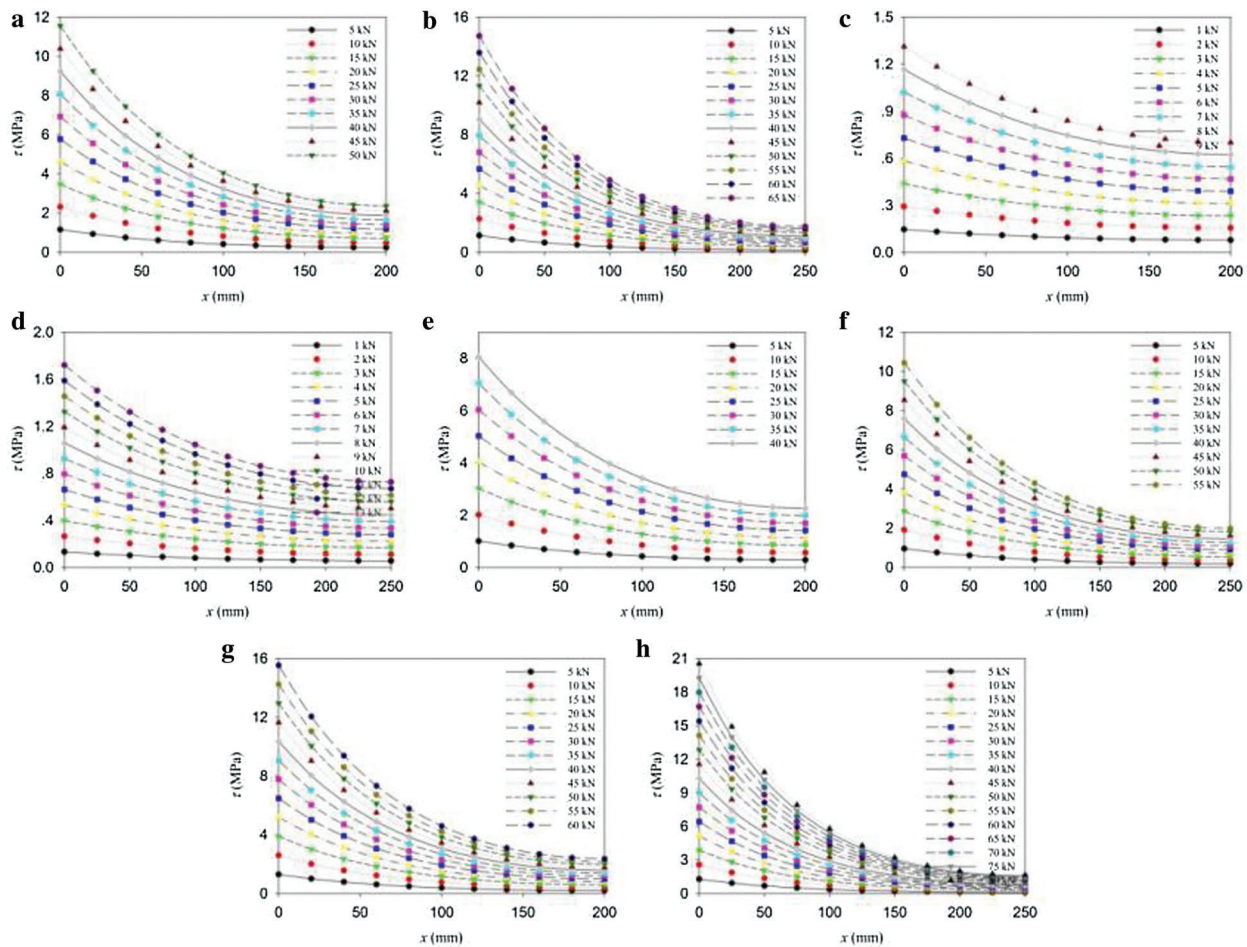
Figure 10: Shear stress distribution of bonding interface along the buried depth for steel bar: (a) A-05; (b) A-06; (c) A-07; (d) A-08; (e) A-09; (f) A-10; (g) A-13; (h) A-14

5 Conclusion

In order to verify the feasibility of newly designed reinforced bamboo scrimber composite (RBSC) beams used in building construction, the bonding properties between steel bar and bamboo scrimber were investigated by anti-pulling tests. Based on the results of sixteen anti-pulling specimens, the main conclusions were obtained as follows:

1. There were two failure modes for anti-pulling tests: (I) the tensile fracture of steel bar; (II) pulling out of steel bar.
2. Both the ultimate load and average shear strength of anti-pulling specimen could be increased greatly with the ribbed bar, high forming density of bamboo scrimber and un-heated bamboo bundle.
3. A theoretical calculation model of the bonding interface between steel bar and bamboo scrimber was developed.
4. The normal stress of bamboo scrimber decreases nonlinearly from the maximum value top to zero, and the shear stress distribution of bonding interface first increase rapidly and then tended to stable with the increase of buried depth.

Conflicts of Interest: The authors declare that they have no conflicts of interest to report regarding the present study.

References

1. Zhong, Y., Wu, G., Ren, H., Jiang, Z. (2017). Bending properties evaluation of newly designed reinforced bamboo scrimber composite beams. *Construction and Building Materials, 143,* 61–70. DOI 10.1016/j.conbuildmat.2017.03.052.
2. Jiang, Z. H. (2007). *Bamboo and rattan in the world*. Beijing: China Forestry Press, 1–50.
3. Li, Z. Y., Wang, D. J., Fan, B. M. (2005). Analysis on status quo and policy of China's bamboo industry. *Journal of Beijing Forestry University (Social Science), 4(4),* 50–54.
4. Albermani, F., Goh, G. Y., Chan, S. L. (2007). Lightweight bamboo double layer grid system. *Engineering Structures, 29(7),* 1499–1506. DOI 10.1016/j.engstruct.2006.09.003.
5. Lakkad, S. C., Patel, J. M. (1980). Mechanical properties of bamboo, a natural composite. *Fibre Science and Technology, 14(4),* 319–322. DOI 10.1016/0015-0568(81)90023-3.
6. Amada, S., Ichikawa, Y., Munekata, T., Nagase, Y., Shimizu, H. (1997). Fiber texture and mechanical graded structure of bamboo. *Composites Part B: Engineering, 28(1–2),* 13–20. DOI 10.1016/S1359-8368(96)00020-0.
7. Li, H. T., Su, J. W., Zhang, Q. S., Deeks, A. J., Hui, D. (2015). Mechanical performance of laminated bamboo column under axial compression. *Composites Part B: Engineering, 79,* 374–382. DOI 10.1016/j.compositesb.2015.04.027.
8. Li, H. T., Wu, G., Xiong, Z. H., Corbi, I., Corbi, O. et al. (2019). Length and orientation direction effect on static bending properties of laminated Moso bamboo. *European Journal of Wood and Wood Product, 77(4),* 547–557. DOI 10.1007/s00107-019-01419-6.
9. Li, H. T., Wu, G., Zhang, Q. S., Deeks, A. J., Su, J. (2018). Ultimate bending capacity evaluation of laminated bamboo lumber beams. *Construction and Building Materials, 160,* 365–375. DOI 10.1016/j.conbuildmat.2017.11.058.
10. Xiao, Y., Yang, R. Z., Shan, B. (2013). Production, environmental impact and mechanical properties of glubam. *Construction and Building Materials, 44,* 765–773. DOI 10.1016/j.conbuildmat.2013.03.087.
11. Correal, J. F., Echeverry, J. S., Ramirez, F., Yamín, L. E. (2014). Experimental evaluation of physical and mechanical properties of Glued Laminated *Guadua angustifolia* Kunth. *Construction and Building Materials, 73,* 105–112. DOI 10.1016/j.conbuildmat.2014.09.056.
12. Correal, J. F. (2008). Mechanical properties of Colombian glued laminated bamboo. *Proceedings of 1st International Conference on Modern Bamboo Structures, ICBS-2007,* 121–127.

13. Chen, F. M., Jiang, Z. H., Wang, G., Li, H., Simth, L. M. et al. (2016). The bending properties of bamboo bundle laminated veneer lumber (BLVL) double beams. *Construction and Building Materials, 119,* 145–151. DOI 10.1016/j.conbuildmat.2016.03.114.

14. Sharma, B., Gatóo, A., Bock, M., Ramage, M. (2015). Engineered bamboo for structural applications. *Construction and Building Materials, 81,* 66–73. DOI 10.1016/j.conbuildmat.2015.01.077.

15. Kumar, A., Vlach, T., Laiblova, L., Hrouda, M., Kasal, B. et al. (2016). Engineered bamboo scrimber: influence of density on the mechanical and water absorption properties. *Construction and Building Materials, 127,* 815–827. DOI 10.1016/j.conbuildmat.2016.10.069.

16. Yu, Y. L., Huang, X. N., Yu, W. J. (2014). A novel process to improve yield and mechanical performance of bamboo fiber reinforced composite via mechanical treatments. *Composites Part B: Engineering, 56(1),* 48–53. DOI 10.1016/j.compositesb.2013.08.007.

17. Li, H. T. (2019). Length and direction effect on the compression performance of parallel bamboo strand lumber. *Journal of Renewable Materials, 7(7),* 583–600.

18. Li, H. T. (2019). Review on connections for original bamboo structures. *Journal of Renewable Materials, 7(7),* 713–730.

19. Li, H. T., Wu, G., Zhang, Q. S., Su, J. W. (2016). Mechanical evaluation for laminated bamboo lumber along two eccentric compression directions. *Journal of Wood Science, 62(6),* 503–517. DOI 10.1007/s10086-016-1584-1.

20. Yu, W. J. (2012). Current status and future development of bamboo scrimber industry in China. *China Wood Industry, 26(1),* 11–14.

21. Shangguan, W. W., Zhong, Y., Xing, X. T., Zhao, R., Ren, H. (2015). Strength models of bamboo scrimber for compressive properties. *Journal of Wood Science, 61(2),* 120–127. DOI 10.1007/s10086-014-1444-9.

22. Shangguan, W. W. (2016). Effects of heat treatment on the properties of bamboo scrimber. *Journal of Wood Science, 62(5),* 1–9. DOI 10.1007/s10086-016-1574-3.

23. Kumar, A., Vlach, T., Laiblova, L., Hrouda, M., Kasal, B. et al. (2016). Engineered bamboo scrimber: influence of density on the mechanical and water absorption properties. *Construction and Building Materials, 127,* 815–827. DOI 10.1016/j.conbuildmat.2016.10.069.

24. Zhou, A. P., Huang, D. S., Li, H. T., Su, Y. (2012). Hybrid approach to determine the mechanical parameters of fibers and matrixes of bamboo. *Construction and Building Materials, 35,* 191–196. DOI 10.1016/j.conbuildmat.2012.03.011.

25. Wei, Y., Ji, X., Duan, M., Li, G. (2017). Flexural performance of bamboo scrimber beams strengthened with fiber-reinforced polymer. *Construction and Building Materials, 142,* 66–82. DOI 10.1016/j.conbuildmat.2017.03.054.

26. Zhang, J. L., Li, Y. S., Liu, R., Xu, D., Bian, X. (2018). Examining bonding stress and slippage at steel-bamboo interface. *Composite Structures, 194,* 584–597. DOI 10.1016/j.compstruct.2018.04.037.

27. Li, Y. S., Zhang, J. L., Liu, R., Zhang, Z. (2017). Study on bond performance of bamboo-steel interface after long-term loading. *Journal of Building Structures, 38(9),* 110–119.

28. Du, M. M., Su, X. Z., Zhao, Y. (2010). Experimental study on bond behavior of ribbed bar and strand. *Journal of Building Materials, 13(2),* 175–181.

29. Mazaheripour, H., Barros, J., Sena-Cruz, J., Pepe, M., Martinelli, E. (2013). Experimental study on bond performance of GFRP bars in self-compacting steel fiber reinforced concrete. *Composite Structures, 95,* 202–212. DOI 10.1016/j.compstruct.2012.07.009.

30. Zhu, R. X., Zhou, Y., Ren, D. H., Yu, Y. L., Yu, W. J. (2011). Effect of manufacturing methods on bamboo fiber based composite performances. *China Wood Industry, 25(3),* 1–3.

31. Zhong, Y., Ren, H. Q., Jiang, Z. H. (2016). Effects of temperature on the compressive strength parallel to grain of bamboo scrimber. *Materials, 9(6),* 436. DOI 10.3390/ma9060436.

32. Qin, L. (2010). *Effect of thermo-treatment on physical, mechanical properties and durability of reconstituted bamboo lumber (Ph.D. Thesis).* Chinese Academy of Forestry, Beijing, China.

33. Zhang, Y. M., Yu, Y. L., Yu, W. J. (2013). Effect of thermal treatment on the physical and mechanical properties of phyllostachys pubescen bamboo. *European Journal of Wood and Wood Products, 71(1),* 61–67. DOI 10.1007/s00107-012-0643-6.